ISSN 1009－3095 *Journal of Zhejiang University*（*SCIENCE*）V.3，No.3，P.272－277，July－Aug.，2002
http://www.periodicals.com.cn；http://www.zju.edu.cn/English

http://www.zjupress.com；http://lib.zju.edu.cn/eindex.htm；jzu_s@mail.hz.zj.cn

Surface treatment of 0Cr19Ni9 stainless steel SMAW joint by plasma melting*

LUO Wei(罗 伟)，LUAN Jing-fei(栾景飞)，YAN Mi(严 密)
(*College of Materials and Chemical Engineering，Zhejiang University，Hangzhou 310027，China*)

Received Jan.21，2001；revision accepted July 16，2001

Abstract: Micro-plasma arc surface melting of 0Cr19Ni9 shielded metal arc welding joint with a micro-plasma arc welder produced a thin surface melted layer with a refined microstructure. The surface treatment changed the anodic polarization behavior in 0.5 mol/L H_2SO_4 solution. The polarization tests showed that for the as-welded joint both the heat-affected zone and the weld metal decreased in resistance to corrosion compared with the as-received parent material while for the micro-plasma arc surface melted joint the corrosion resistance increased significantly. This increase in corrosion resistance is attributed to the rapid solidification of the melted layer. Rapid solidification of the melted layer refines its microstructure，decreases its microsegregation，and inhibits the precipitation of chromium carbides at the grain boundaries.

Key words: Surface melting，Stainless steels，Plasma arc，Welding joint
Document code: **CLC number:** TG 174.4

INTRODUCTION

0Cr19Ni9 unstabilized austenitic stainless steel is widely used for many applications. It can be readily fabricated by arc welding. Shielded metal arc welding（SMAW）is one of the commonly used processes（Luo，1996）. The weldments manufactured from this material generally behave differently from the parent material in corrosion resistance. For the heat-affected zone（HAZ）the corrosion resistance mainly depends upon the type of welding，and welding parameters such as welding current and welding speed. For the weld metal the corrosion resistance is dependent upon the type of welding，the type of filler metal，and other welding conditions. The corrosion resistance of arc welding joints in the as-welded condition usually is lower than that of the as-received parent steel.

Surface modification is one way to improve welding joints surface resistance to corrosion. Laser surface melting（LSM）can produce a rapidly solidified surface layer on metals and alloys，therefore，it can modify the surface microstructure and hence affect surface-related properties such as corrosion resistance and wear resistance（Li et al.，1996；Tassin et al.，1996；Yan et al.，1996）. Similar to LSM，because of the high energy density，the small diameter，and the low heat input of the arc beam，micro-plasma arc（MPA）can be used in the surface modification of metals and alloys（Yan et al.，1997；Luo et al.，1999）. While there were a number of studies on the influence of LSM in modifying the microstructure and properties of metals and alloys（Yan et al.，1996；Rao et al.，1993；Huang，et al.，1996），but few on the surface modification by MPA surface melting.

The main purpose of this work was to study the corrosion resistance of 0Cr19Ni9 stainless steel SMAW joint and to investigate whether a rapidly solidified surface layer could be produced on the joint by MPA surface melting. The microstructure and corrosion resistance of the joints with and without MPA surface melting are discussed in this paper.

* Project supported by Zhejiang Provincial Science & Technology Foundation（No.001101112）and Cao Guang-Biao High Science & Technology Foundation of Zhejiang University（No.223296078013），China

EXPERIMENTAL PROCEDURES

0Cr19Ni9 steel plate in the as-received condition containing (wt.%) C 0.06, Cr 18.3, Ni 9.15, Mn 0.68, Si 0.59, S 0.012, P 0.029 and the balance iron with dimensions 40 cm×20 cm×1.0 cm was machined to have a V-groove with depth of 0.4 cm and groove angle of 60° on its front surface. Then the plate was welded on the V-groove by SMAW process with Type E0-19-10Nb-16 covered electrode containing (wt.%) C 0.05, Cr 20.05, Ni 9.9, Mn 1.84, Si 0.53, S 0.004, P 0.018, Nb 0.58, Cu 0.05, Mo 0.03 and the balance iron. Before welding, the surface to be welded was cleaned with acetone. After machining the reinforcement flush with the plate surface, and cleaning, the surface of the welded joint was scanned by MPA using a modified MPA welder-WLA-10B MPA welder. The distance between the nozzle of the plasma arc torch and the specimen was about 3.0 mm. The main parameters for the welding process and MPA melting are listed in Table 1. In order to achieve area coverage successive passes of the sample were made in which the overlap between the resultant MPA melted tracks was about 20%.

Table 1 Main parameters of the welding and MPA surface melting

Welding process Parameters	Conditions	MPA melting Parameters	Conditions
Filler metal	E0-19-10Nb-16 ϕ 4.0mm	Plasma gas flux (Ar) Shielded gas flux (Ar)	800 ml/h 900 ml/h
Welding current	160 A	Melting current	4 A
Arc voltage	23 V	Travel speed	150 mm/min
Welding speed	170 mm/min	Arc beam diameter	2 mm
Polarity	DCRP[a]	Polarity	DCSP[b]

[a] DCRP = direct current reversed polarity; [b] DCSP = direct current straight polarity

Microstructural characterization was carried out by optical microscopy (OPM) following etching with 5 ml HCl + 100 ml C_2H_5OH + 1g $C_6H_3N_3O_7$ and by scanning electron microscopy (SEM). Phase identification was carried out by X-ray diffraction (XRD). Corrosion behavior was studied by means of potentiodynamic anodic polarization test in 0.5mol/L H_2SO_4 solution prepared with analytical grade reagent and distilled water. The samples prepared for polarization tests were spark-cut from the joint with and without MPA remelting as illustrated in Fig. 1. Only one sample surface with area of about 2.5 – 3.0 cm^2 was exposed to the electrolyte, the other surfaces were covered with epoxy resin. The boundary between the sample and the epoxy resin was sealed with paraffin wax to avoid crevice corrosion. The polarization tests were carried out using a conventional three-electrode cell, comprising the sample, a platinum foil counterelectrode and a saturated calomel reference electrode. A HDV-7C transistor potentiostat was used to control the potential at a sweep rate of 10 mv/min. Before polarization the sample was immersed in 0.5 mol/L H_2SO_4 solution for 10 minutes to stabilize the open circuit potential. All potentials are quoted with respect to the saturated calomel electrode scale. For comparison, the same corrosion test was carried out under the same experimental conditions on the parent plate sample in the as-received condition.

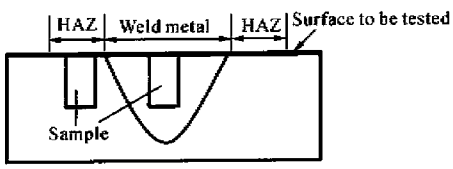

Fig. 1 Sample positions for polarization tests of the joint

RESULTS AND DISCUSSION

1. Corrosion resistance of the weld metal

Anodic polarization curves in 0.5 mol/L H_2SO_4 solution for the 0Cr19Ni9 steel in the as-received condition and for the joint samples in the as-welded and MPA surface melted conditions are shown in Fig. 2. The electrochemical data measured in the tests are listed in Table 2. The corrosion resistance of the as-deposited weld metal of the austenitic stainless steel arc-welding joint mainly depended upon

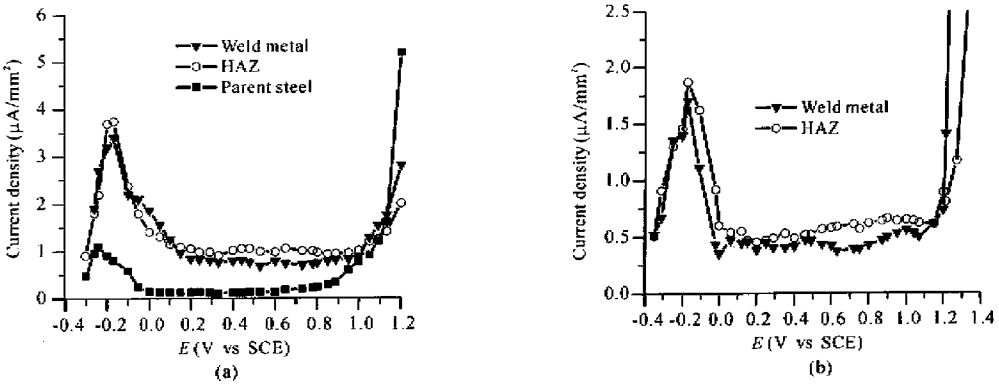

Fig. 2 Anodic polarization curves of the samples in 0.5mol/L H_2SO_3 solution
(a) without melting; (b) with melting

Table 2 Anodic polarization experimental results for samples with and without surface melting

Sample	Critical current density for passivity($\mu A/mm^2$)	Passive current density($\mu A/mm^2$)	Transpassive potential(V)	Primary passive potential(V)	Passive potential range(V)
As-received parent steel	1.12	0.13－0.15	0.88	－0.233	0.013－0.88
Weld metal before melting	3.49	0.90－1.12	1.05	－0.16	0.10－1.05
HAZ before melting	3.76	1.15－1.35	1.25	－0.20	0.10－1.25
Weld metal after melting	1.70	0.38－0.54	1.10	－0.17	－0.02－1.10
HAZ after melting	1.87	0.45－0.75	1.23	－0.17	0.06－1.10

such factors as composition and structure. In as-received condition, commercial 0Cr19Ni9 steel normally has excellent weldability, provided it is welded with matching filler metal which yields an austenitic weld metal with about 4－12% delta ferrite contents (Zhou et al., 1992). The weld metal with fully austenitic solidification shows strong hot cracking sensitivity. To obtain high hot cracking resistance, the weld metal structure produced should not be fully austenitic but rather austenitic with a delta ferrite content. It was proved that weld metal with about 5% ferrite exhibits desirable resistance to intergranular corrosion (IC) in practical applications (Zhou et al., 1992; Folkhard, 1991). In the present case of welding 0Cr19Ni9 by SMAW process, it can be predicted from the chemical compositions of the covered electrode and the base metal using the Schaeffler diagram that the as-welded structure of the weld metal which has high or low dilution with the

base metal during welding is austenitic weld metal containing about 4 − 8% delta ferrite. The corrosion of the austenitic stainless steels is mainly related to the chromium carbide precipitation at the grain boundaries. This precipitation leads to the chromium depletion in the zones in the immediate vicinity of the grain boundaries. The chromium depleted zones become susceptible to corrosion. Rising carbon contents and rising welding heat input facilitate this precipitation, but the alloying element niobium reduces this precipitation and hence limits the susceptibility to IC. In the present work, the niobium stabilized E0-19-10Nb-16 covered electrode and the unstabilized parent metal 0Cr19Ni9 have relatively high carbon contents, leading to the high carbon contents in the deposited weld metal. The precipitation of chromium carbides in the weld metal would not be inhibited completely due to the insufficient quantity of niobium. In addition, the formation of TiN in the weld metal reduces the purity of the weld, leading to the decrease in resistance of the weld metal to corrosion (Editorial Board, 1991), thus the corrosion resistance of the weld metal in the as-welded state decrease compared with the as-received parent steel. And finally, to a certain extent, the decrease in corrosion resistance is attributed to the segregations and welding defects in the deposited weld metals as well.

2. Corrosion resistance of the HAZ

During welding, heating of the parent material takes place in the HAZ. The material in the HAZ is heated to a variety of temperatures range from ambient temperature to the melting range of the alloy in question. Thus, the HAZ will generally behave differently from the parent steel in corrosion resistance. In the present case, with the effect of heat input during welding, "weld decay"is present in the HAZ. The metal in the weld decay zone is heated for a sufficient time within the temperature range of about 600 to 1000℃, known as sensitizing temperature range, during welding, to precipitate intergranular carbides. Thus, the weld decay zone becomes susceptible to IC, the amount of precipitation or degree of sensitization was approximately proportional to the carbon content of the austenitic steel. It was the high carbon content of 0Cr19Ni9 steel (up to 0.06 wt.%) that degraded the corrosion resistance of the as-welded HAZ compared with the as-received parent steel.

Three methods are used to control or minimize IC of austenitic stainless steels: (1) employing high-temperature solution heat treatment, commonly termed quench-annealing or solution-quench, (2) adding elements that are strong carbide formers such as titanium and niobium, and (3) lowering the carbon content to below 0.03% (Fontana, 1986). In the present work, the deposited weld metal and HAZ metal had almost the same carbon contents but the former contains stabilizing element niobium due to the stabilized covered electrode E0-19-10Nb-16, so it showed slightly higher resistance than the latter to corrosion. In addition, the coarse grains in the HAZ had negative influence on its corrosion resistance.

Compared with the HAZ, weld metal is not generally considered to be so susceptible to IC. In weld metal, carbide precipitation occurs more uniformly throughout the structure at the interphase or substructure boundaries rather than the grain boundaries, so that the degree of chromium depletion along the grain boundaries is lower than that in the HAZ. This is consistent with the results shown in Fig. 2 and Table 2.

3. Influence of the MPA surface melting on the corrosion resistance of the joint

For the MPA melted samples the corrosion resistance improved considerably compared over that of the samples without surface melting. The surface melting produced a tiny molten pool on the surface of the substrate so the chromium carbides precipitated in both the HAZ and the weld metal during welding were dissolved in the molten metal and a more homogeneous alloy was obtained. After the MPA was withdrawn, the non-melted substrate could rapidly cool the molten metal on the surface of the substrate to room temperature to form a resolidificated layer. The thickness of the layer was dependent upon the arc heat input. In the present case the layer was

about 110μm thick (Fig. 3). As a result, the thin layer was in the molten state and in the high temperature range for a shorter time so that the diffusion of elements was inhibited, leading to the inhibition of chromium carbide precipitation and the microsegregation of such elements as sulfur, phosphorus and silicon in the grain boundaries. The segregation of such elements in the grain boundaries increased the danger of IC attack (Folkhard, 1991; Editorial Board, 1991). In addition, the layer resolidification under very high rate of cooling resulted in a very fine microstructure as shown in the SEM image (Fig. 4). The fine crystalline grains facilitated formation of a Cr_2O_3 passive film (Baer, 1973). Thus, the resistance of the melted layer to corrosion would be improved significantly by the MPA surface treatment.

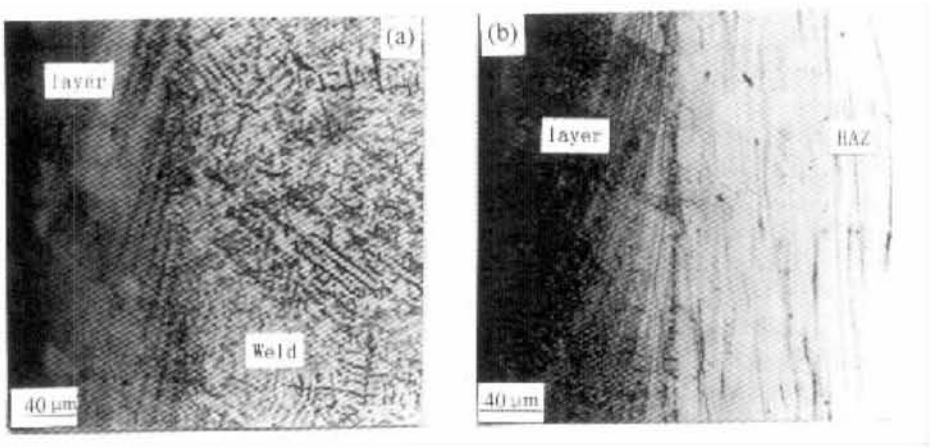

Fig. 3 Micrograph of the cross-section of the MPA melted layer on
(a) the weld; (b) the HAZ

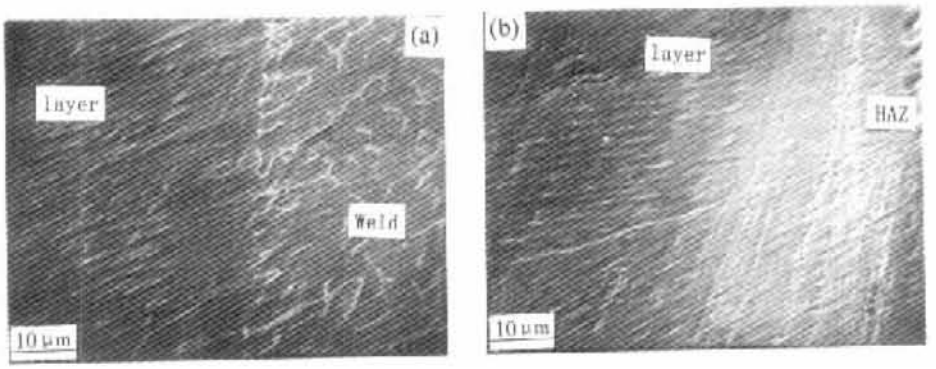

Fig. 4 Scanning electron micrograph of the cross-section of the MPA melted layer on
(a) the weld; (b) the HAZ

Finer structure could be observed in the region closer to the substrate. In the region closer to the top surface, because the solidification speed was low and the temperature gradient was small compared to the region closer to the substrate, the structure was composed of cellular dendrite crystals as shown in Fig. 5. The melted layer was composed of austenite (γ) and ferrite (δ) as shown by XRD analysis (Fig. 6). No chromium carbide was detected, suggesting its precipitation at the grain boundaries in the layer during solidification would be inhibited effectively as a result of the high cooling rate.

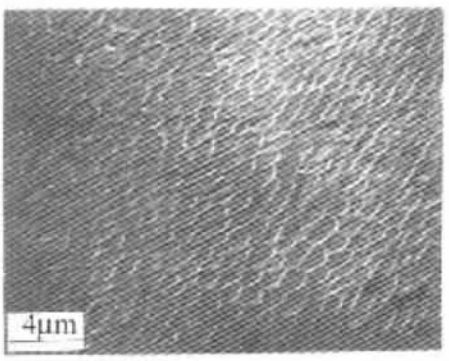

Fig.5 Scanning electron micrograph of the surface of the MPA melted layer

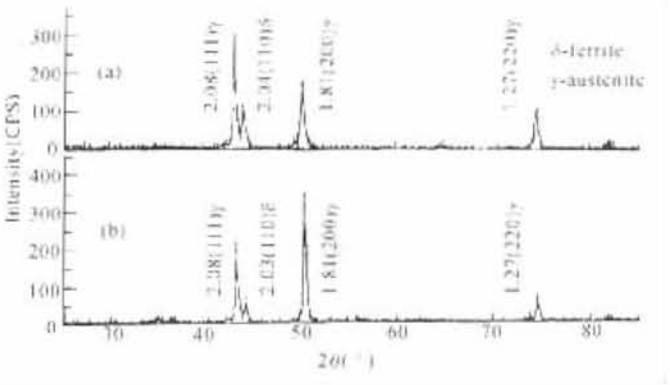

Fig.6 XRD spectra of the MPA melted layer on (a) the Weld and (b) the HAZ

CONCLUSIONS

1. Due to the effect of the heat input during welding operation, the localized sensitization of the HAZ of 0Cr19Ni9 SMAW joint decreased its corrosion resistance. In addition, the presence of coarse grains in certain region of the HAZ had negative effect on the resistance.

2. For the weld metal in the as-welded condition the joint decreased in corrosion resistance compared with the as-received parent steel. This is attributed to the chromium carbide precipitation as a result of insufficient quantity of stabilizing element niobium, and relatively higher carbon content of the covered electrode used.

3. MPA surface melting of the 0Cr19Ni9 SMAW joint yielded a modified microstructure consisting of austenite (γ) and cellular ferrite (δ) and/or cellular dendrites. Rapid melting, and solidification of the melted layer on the surface of the welding joint inhibited the precipitations of the chromium carbide and decreased the microsegregations of elements in the layer, leading to the increase in corrosion resistance of the welding joint.

References

Baer, D. R., Merz, M. D., 1980. Differences in oxides on large and small grained 304 stainless steel. *Metall. Trans*, **11A**: 1973.

Editorial Board of Essentials of Advanced Mater. for High Technology, 1991. Essentials of advanced materials for high technology. Chinese Sci. and Tech. Publishing House, Beijing, p. 239 (in Chinese).

Folkhard, E., 1991. Welding metallurgy of stainless steels. Springer-Verlag World Publishing Corp., p. 436.

Fontana, M. G., 1986. Corrosion engineering. McGraw-Hill Book Company, p. 127.

Huang, C. C., Tsai, W. T., Lee, J. T., 1996. Surface modification of carbon steel with laser treated nitrogen-containing stainless steel layers. Surf. Coat. Tech., **79**: 67.

Li, R., Ferreira, M. G. S., Almeida, A., Vilar, R., Watkin, K. G. and McMahon, M. A., 1996. Localized corrosion of laser surface melted 2024-T351 aluminum alloy. *Surf. Coat. Tech.*, **81**: 290.

Luo, W., Zhang, X. B., 1999. Effect of micro-plasma arc surface remelting on the corrosion resistance of 1Cr18Ni9Ti. *Materials Protection*, **32**: 13 (in Chinese).

Luo, W., 1996. Welding technique of air separating plant. *Cryonetics*, **6**: 10 (in Chinese).

Rao, D. R. K., Venkataraman, B., Asundi, M. K., Sundararajan, G., 1993. The effect of laser surface melting on the erosion behaviour of a low alloy steel. *Surf. Coat. Tech.*, **58**: 85.

Tassin, C., Laroudie, F., Pons, M., Lelait, L., 1996. Improvement of the wear resistance of 316L stainless steel by laser surface alloying. *Surf. Coat. Tech.*, **80**: 207.

Yan, M., Zhang, X. B. and Zhu, W. Z., 1996. The microstructure and wear resistance of plasma-arc remelted Ni-Base overlay. *J. Mater. Sci. Lett.*, **15**: 2038.

Yan, M., Zhu, W. Z., 1997. Surface treatment of 45 steel by plasma-arc melting. *Surf. Coat. Tech.*, **91**: 183.

Yan, M. and Zhu, W. Z., 1998. A new approach of surface treatment: remelting of micro-beam plasma arc. *J. Mater. Sci. Lett.*, **34**: 222.

Zhou, Z. F., Zhang, W. Y., 1992. Welding metallurgy and weldability of metals. Engineering Industry Publishing House, Beijing, p. 169.